NILU
OPPDRAGSRAPPORT NR 18/79
REFERANSE: 25077
DATO: JUNI 1979

A MODEL FOR HEAVY GAS DISPERSION IN THE ATMOSPHERE

BY

K.J. EIDSVIK

NORWEGIAN INSTITUTE FOR AIR RESEARCH
P.O. BOX 130, N-2001 LILLESTRØM
NORWAY

ISBN 82-7247-113-2

SUMMARY

A simple model for the dispersion of heavy and cold gas clouds is developed. The horizontal dimension of the cloud is assumed to increase due to the gravity fall of the cloud. The cold cloud is heated from below and from air entrainment. The initial entrainment velocity is assumed to be linearly proportional to the front velocity and decay as the square of it. The entrainment at the upper surface is estimated as for atmospheric inversions and density interfaces in laboratory flows. The model predictions are shown not to be critically dependent on coefficient variations. Experimental data on heavy gas dispersion are predicted accurately.

The hazard of heavy gas clouds is predicted to be dependent on environmental conditions, particularly the roughness of the underlying surface and the mean wind speed. Under unfavourable conditions a heavy gas cloud from a major "instantaneous" release may be hazardous for hours several kilometers from the source.

TABLE OF CONTENTS

A MODEL FOR HEAVY GAS DISPERSION IN THE ATMOSPHERE

1 INTRODUCTION

1.1 The Problem

The production, transportation and storage of large quantities of heavy, explosive or poisonous gases may present serious hazards to the public. A cloud of methane, propane or butane may be flammable if the mean volume concentration is higher than approximately 1%. A cloud of chlorine may be poisonous at concentrations of approximately 10^{-5}%. If accidental release occurs in unfavourable atmospheric flows, the resulting cloud could be hazardous far away from the source. Several investigations have been done towards estimating the spread of such clouds, (Fay (1), van Ulden (2), te Riele (3), Germeles and Drake (4),(5), Eidsvik (6) and Kaiser and Walker (7)). Experiments involving the release of heavy gas clouds are described by Burges et al. (8), Feldbauer et al. (9),(10) and in (2). Resent experiments at Porton, described by Picknett (11) have contributed substantially to additonal relevant data. Most of the proposed models are very simple and all involve uncertain ad hoc assumptions. Although the authors may claim that their models fit the data, the fit could easily be caused by the incomplete, sparse and stochastic data, and the number of coefficient used for curve fitting. We will show that our model, (6), can predict important aspects of heavy gas spreading as revealed by the Porton data, with adjustment of only one coefficient for initial entrainment.

1.2 Outline of the process

The gas if often stored in liquified form. When this liquid is exposed to normal environments, the gas may boil off from a liquid pool at a boiling temperature that may be much lower than the environmental temperature. A significant fraction of the liquid may be thrown into the air-gas cloud as droplets to evaporate there. If the characteristic time required to release

most of the gas is t_r, and the characteristic radial gas cloud speed during the release is U_g, the cross wind dimension of the cloud at the time t_r is $r_2(t_r) \simeq U_g t_r$. With a transport velocity, U_a, which may be somewhat less than the atmospheric wind speed, the alongwind dimension of the cloud at time t_r become $r_1(t_r) \simeq (U_g + U_a)t_r$. When $U_a << U_g$, the cloud is approximately cylindrical at t_r. In this case ("instantaneous source"), the subsequent spread will be reasonably isotropic in the horizontal plane. For a given t_r, this idealisation is most realistic under weak mean wind conditions. When $U_a >> U_g$, the cloud has much larger longitudinal than transverse dimension at t_r. In this case ("continuous source") the most important horizontal spread direction will be the transverse. For a given t_r, this idealization is most realistic for high mean wind conditions. Unless otherwise stated in what follows, the source is assumed to be instantaneous. Experimental evidence suggests that the spread from an instantaneous heavy gas source may conveniently be discussed in terms of a rapid phase of initial slumping, an intermediate phase of less vigorous development, and finally a phase of passive scalar diffusion.

If the gas release is sufficiently rapid, the initial phase is characterized by a vortex ring at the pheriperial cloud boundary. In the Porton experiments it is estimated that a significant fraction of the gas mass is contained in this vortex ring (11). The characteristic duration of this phase is t_I. Both the characteristic time for the duration of a realistic gas release, t_r, (1,2,4,5) and time for the slumping and heating of a cold cloud, t_I, are probably of the same order of magnitude. The release or initial air entrainment has been estimated as significant in various experiments (2,7,11). A physically realistic modelling of the initial phase would be extremely difficult because it involves nonequilibrium boiling and nonequilibrium thermal interaction between two complicated turbulent flows. A reasonably realistic model for the gas flow alone would probably require a very complicated turbulence model of the type discussed by Donaldson and Bilanin (12) or Deardorff (13). As the initial mean gas flow is definitely three-dimensional and of small scale, a very small grid size would be necessary along all spatial di-

rections over a large spatial domain. With todays computers such a model would not be feasible. In addition the model would be uncertain due to uncertain closure schemes. It is instead hoped that a simple ad hoc model can predict the approximate bulk properties of the cloud at the end of the initial phase.

For the intermediate stage, $t \geq 0(t_I)$, the gas mixture is still denser than air and continues to spread radially due to gravity. Because of surface stress and heat transfer, it is probably a well developed turbulent flow. The turbulence is likely to give a reasonably homogeneous air-gas mixture inside the cloud. The horizontal dimension of the cloud, r, is much larger than the height, h. Assumed representative properties of a vertical cross section of the flow are shown in Figure 2.1. The assumed mean profiles at the upper cloud boundary suggest that the flow may

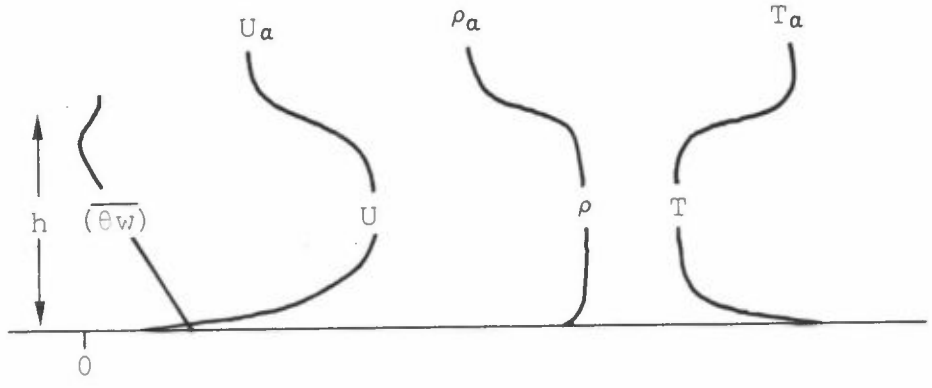

Figure 2.1: Assumed, representative vertical profiles of the "intermediate" heavy gas flow.

h - characteristic vertical dimension
U - " mean velocity vector
ρ - " mean density
T - " mean temperature
$\overline{\theta w}$ - " vertical temperature flux
θ - " fluctuating temperature
w - " " vertical velocity

be subject to Kelvin Helmolz instability. This instability would imply an effective dilution of the gas cloud. For $t > t_I$ it is assumed that the flow adjusts its gradient Richardson number over the interface so that Kelvin Helmholz instability is almost always avoided. If the above concepts of the flow are realistic, the dispersion can not be realistically estimated by using K-theories of turbulence as done in references (3) and (5). In the bulk cloud there will be large vertical turbulent transports in spite of negligible mean gradients, and across the large mean gradients ("interface") the turbulent transport may be small. It would also be difficult to use numerical models of the Reynolds equations for mean flow computations as done in reference (13), because the resolution of the grid would have to be very small in the neighbourhood of the cloud boundaries. Our model is mainly meant to be applicable for this intermediate stage of cloud development.

As the density difference between the cloud and atmosphere vanishes, the dispersion must approach that of a passive scalar cloud. At this stage the gas concentration has decreased considerably so that the dispersion may not need to be estimated accurately. Sufficient accuracy may be achieved by designing the heavy gas model to have an approximately correct limiting behaviour as the density difference vanishes.

2 A DISPERSION MODEL FOR A HEAVY GAS CLOUD

2.1 Mass of gas mixture

With the assumption of a reasonably well defined boundary of the gas mixture, the mass of the cylindrical cloud is :

$$\pi\rho(t)\cdot r^2(t)\cdot h(t) = M_g + M_a(t) \qquad (2.1a)$$

Here M_g is the mass of the released gas and $M_a(t)$ is the mass of entrained air.

For a continuous source, the corresponding equation is obtained by considering the flux of gas mixture at a distance $x = U_a \cdot t$ from the source

$$U_a \, \rho(x) \, 2r(x)h(x) = \frac{dM_g}{dt} + \frac{dM_a}{dt} \qquad (2.1b)$$

Here 2r is the transverse dimension of the plume $\frac{dM_g}{dt}$ is the source strength, and $\frac{dM_a}{dt}$ is the entrained air over the distance x.

As the density difference becomes small and the "interface" vanishes, h and r may still be identified as characteristic cloud dimensions.

2.2 Gravity induced velocity

The frontal speed of a frictionless heavy gas flow has been estimated by several authors (1,2,4), to be

$$\frac{dr}{dt} = U_g = \alpha_1 \, (gh \, \frac{\Delta\rho}{\rho})^{\frac{1}{2}} \qquad (2.2)$$

Here $\alpha_1 \simeq 1.3$ is a coefficient, g is the acceleration of gravity, and $\Delta\rho=\rho-\rho_a$ with $\rho_a=\rho_a(z)$ the density of the atmosphere. When there are no horizontal variations of h and ρ, the gravity induced radial horizontal speed will vary linearly with the distance from the centre of a circular cloud. The average gravity speed over the area of a circular cloud then becomes $\frac{2}{3} U_g$. The average gravity speed across a plume is $\frac{1}{3} U_g$, This spatial distribution of velocity inside the cloud, some vertical momentum exchange and continuity, suggest that there should be a tendency for a vortex ring of the correct circulation direction to form above the cloud front. With momentum exchange, there would also have to be a mass exchange. However, neither need probably be large for the spectacular vortex ring to be visible.

With negligible heat transfer. Equations (2.1a) and (2.2) give the same horizontal spreading for the two extreme situations: no entrainment, and $\Delta\rho/\rho \to \Delta\rho/\rho_a \to 0$. This indicates what is later shown by numerical integrations; that the increase of the horizontal cloud dimension is almost independent of the entrainment process. The limit $\Delta\rho/\rho \simeq \Delta\rho/\rho_a \to 0$ occurs when $t >> t_I$ and is of most interest here. As $\Delta\rho/\rho_a \to 0$ there will be negligible temperature differences so that the increase in cloud volume, $V(t)$, is only caused by entrainment. Equation (2.1a) may then be written as:

$$V(t)\rho(t) = V(t_o)\rho(t_o) + (V(t) - V(t_o))\rho_a \qquad (2.3)$$

with t_o a reference time. Rearrangements give:

$$\frac{\Delta\rho(t)}{\rho_a} \simeq \frac{\Delta\rho(t_o)}{\rho_a}\,\frac{V(t_o)}{V(t)} = \frac{\Delta\rho(t_o)}{\rho_a}\,\frac{V(t_o)}{\pi r^2 h} \qquad (2.4)$$

Introducing (2.4) into Equation (2.2), gives the following simple relation:

$$r\frac{dr}{dt} = \alpha_1 \left(\frac{g\,V(t_o)}{\pi}\,\frac{\Delta\rho(t_o)}{\rho_a}\right)^{\frac{1}{2}}$$

$$= \left(r\frac{dr}{dt}\right)_{t_o} = \left(\frac{d\,\frac{1}{2}r^2}{dt}\right)_{t_o} = \text{const.} \qquad (2.5)$$

It is easily seen that the same type of equation would have been obtained if cloud volume and density were conserved (2). Integration of Equation (2.5) gives:

$$r^2(t) = r^2(t_o) + \left(r\frac{dr}{dt}\right)_{t_o}(t-t_o) \qquad (2.6)$$

When $t >> t_I$, the horizontal gravity spread does therefore approach the same type of law as that of a large passive scalar cloud. The dispersion of a passive scalar cloud is discussed by for instance Monin and Yaglom (14). Its horizontal dimension, characterized by the variance, increases with the time approximately as:

$$\frac{dEr^2}{dt} \simeq \begin{cases} \sigma_u (U_a L)^{-1/3} t^2, & \text{for } (Er^2)^{\frac{1}{2}} << (U_a L) \\ 4 \sigma_u{}^2 L, & \text{for } (Er^2)^{\frac{1}{2}} >> (U_a L) \end{cases} \qquad (2.7)$$

Here σ_u is the standard deviation of an atmospheric horizontal velocity component, and L is the Lagrangian integral scale. If the gravity flow and the effects of atmospheric turbulence can be considered to be independent, the gravity effect dominate the diffusion as long as

$$\frac{dr^2}{dt} = \left(\frac{dr^2}{dt}\right)_{t_o} > \begin{cases} \sigma_u (U_a L)^{-1/3} t^2 & \text{for } r(t_o) << U_a L \\ 4 \sigma_u{}^2 L & \text{for } r(t_o) >> U_a L \end{cases} \qquad (2.8)$$

For the most hazardous, large clouds, this give

$$\left(\frac{dr}{dt}\right)_{t_o} > 2 \left[\frac{U_a L}{r(t_o)}\right] \sigma_u \qquad \text{for } r(t_o) >> U_a L \qquad (2.9)$$

Since σ_u is usually much less than U_a, the turbulent dispersion is predicted not to dominate unless σ_u is significant larger than the gravity velocity at t_o. In reality the turbulent (and laminar) friction will probably reduce the effectiveness of the organized gravity flow. Lacking a theory for this interaction, it is assumed that Equation (2.2) describes the horizontal spread without explicit modifications for atmospheric turbulence. As shown, it has at least the correct limiting shape for large clouds as the density difference vanishes.

2.3 Entrainment of air

From experiments (2,11) it appears that for times $t \leq 0(t_I)$ and $t > 0(t_I)$ the entrainment is dominated by two different laws. The initial gas flow may be very complicated and highly dependent upon the details of the release process. The vortex ring near the cloud front seems to be important, implying that the entrainment at this stage occurs over an area of the same order of magnitude as the frontal area. The entrainment velocity is $(\frac{dr_d}{dt})$.

$$\frac{dM_a}{dt} \rightarrow \rho_a \, 2\pi r h (\frac{dr_d}{dt}), \qquad \text{for } t < 0\ (t_I) \tag{2.10}$$

Later, as the vortex is dissipated, entrainment is expected to be most important at the large upper surface of the cloud. The entrainment velocity is $(\frac{dh_d}{dt})$

$$\frac{dM_a}{dt} \rightarrow \rho_a \pi r^2 (\frac{dh_d}{dt}), \qquad \text{for } t > 0(t_I) \tag{2.11}$$

The total air entrainment is the sum of the two.

$$\frac{dM_a}{dt} = \rho_a \pi r^2 \left[\frac{dh_d}{dt} + 2\,\frac{h}{r}\,\frac{dr_d}{dt}\right]$$

$$= \rho_a \pi r^2 (\frac{dh}{dt})_* \tag{2.12a}$$

It is assumed that $(\frac{dr_d}{dt})$ decreases fast enough so that Equation (2.12a) approaches Equation (2.11) as $t > 0(t_I)$.

For the continuous source case, the corresponding equation is obtained by considering the entrainment flux.

$$\frac{dM_a}{dt} = \rho_a \left[\int_0^x (2r)(\frac{dh_d}{dt})\, dx + \int_0^x (2h)(\frac{dr_d}{dt})\, dx\right] \tag{2.13}$$

Differentiation with respect to x gives

$$\frac{d}{dx}\left(\frac{dM_a}{dt}\right) = 2\,\rho_a r\left[\frac{dh_d}{dt} + \frac{h}{r}\,\frac{dr_d}{dt}\right]$$

$$= 2\,\rho_a r\left(\frac{dh_d}{dt}\right)_* \qquad (2.12b)$$

2.3.1 Initial

The "traditional" ad hoc peripheral entrainment velocity is

$$\frac{dr_d}{dt} = \alpha_5\, U_g \qquad (2.14)$$

For models to fit different data it is necessary that the magnitude of α_5 varies considerably. With the large initial entrainment required to satisfy the Porton data, $\alpha_5 \in (0.5,1)$, it is found that Equation (2.14) results in the following undesirable properties: a) The result depend critically on the choice of α_5. b) Peripheral entrainment does normally dominate at all stages of the cloud development. The former implies that an uncertain result is estimated by means of a complicated method, while the latter at best makes the model inconsistent. These unwanted properties are, to a large extent, avoided if the initial entrainment velocity is assumed to be proportional to $U_g^{\,p}$, with $p > 1$. Choosing the simplest, quadratic alternative, $p = 2$:

$$\frac{dr_d}{dt} = \frac{\alpha_5}{U_g(0)}\,U_g^{\,2}(t) \qquad (2.15)$$

Numerical simulations show that the objectionable properties a, and b, are now removed. Our initial entrainment velocity is thus equal to the "traditional" peripheral entrainment velocity. However, as the time goes on, it is reduced by a factor of $U_g(t)/U_g(0)$.

3.2.2 Vertical

Provided that the velocity shear near the upper boundary of the cloud does not have a decisive effect on the entrainment, the entrainment at the upper boundary may be estimated from models on "density interface" flows as for instance discussed by Kato and Phillips (15), Crapper and Linden (16), Wu (17), Tennekes (18), Heidt (19), Zeman and Tennekes (20) and Long (21,22). The estimated velocity entrainment may differ somewhat from one author to another. With the uncertainties associated with heavy gas flow, we seek a simple relation with parsimonious use of experimental coefficients. It is also desirable that the entrainment approaches the approximately correct value for a passive scalar cloud as the density difference vanishes. The Zeman-Tennekes type of entrainment equation fulfils these requirements.

$$\frac{dh_d}{dt} = \frac{\alpha_4}{\alpha_6^* + R_i} w \qquad (2.16)$$

Here w is a characteristic vertical turbulent velocity and R_i is the Richardson number

$$R_i = \frac{gh \frac{\Delta\rho}{\rho}}{w^2} \qquad (2.17)$$

The coefficient α_4 is chosen so that the entrainment velocity becomes equal to the Kato and Phillips law (15) for large Richardson numbers and $\alpha_6^* = \alpha_4/\alpha_6$, so that the entrainment approaches the approximately correct limiting value as the effect of the density difference vanishes, i.e. as $R_i \to 0$:

$$\frac{dh_d}{dt} = \alpha_6 w \qquad \text{as} \quad R_i \to 0 \qquad (2.18)$$

According to Tennekes and Lumley (23), this equation describes the approximate growth rate of a neutral boundary layer when $\alpha_6 \simeq 0.3$. The entrainment equation for the heavy gas flow does, therefore, contain only one independent coefficient.

It seems physically reasonable that the convective and mechanical turbulence w_T and w_m respectively should affect the entrainment differently (6,13). We choose what seems to be a simple alternative for estimating the combined entrainment effect:

$$w^2 = (\alpha_2 \, w_T)^2 + (\alpha_3 \, w_m)^2 \qquad (2.19)$$

The convective and mechanical velocities are well established as

$$w_T = \left((\overline{\theta w})_0 \, \frac{gh}{T} \right)^{1/3} \qquad (2.20)$$

$$w_m = u_* = \left(\frac{1}{2} \, c_f\right)^{\frac{1}{2}} U \qquad (2.21)$$

respectively, where c_f is the "surface drag coefficient". In connection with heavy gas dispersion, c_f is considered as an environemental variable rather than as a coefficient. Kitaigorodskii (24) has estimated $c_f \simeq 2 \cdot 10^{-3}$ to be a representative value over water. Over a smooth land surface it is significantly larger. U is a representative "free stream" velocity for the cloud approximated as the quadratic mean of the average gravity flow and wind speed

$$U^2 \simeq \begin{cases} \left(\frac{2}{3} \, U_g\right)^2 + U_a^2, & \text{"instantanuous"} \\ \left(\frac{1}{3} \, U_g\right)^2 + U_a^2, & \text{"continuous"} \end{cases} \qquad (2.22)$$

When Equation (2.19) is substituted into Equation (2.16) the coefficient α_3 (or α_2) may be included into α_4 so that only one new independent coefficient is introduced. This coefficient characterizes the difference between convective and mechanical entrainment.

In the limit as $t >> t_I$, the heat transfer must be small and the governing parameter for the entrainment, the Richardson number, is obtained by substituting from Equations (2.2), (2.21) and (2.22) into Equation (2.17):

$$R_i = \frac{U_g^2}{\alpha_1^2 (\frac{1}{2} c_f) \left((\frac{2}{3} U_g)^2 + U_a^2 \right)} \tag{2.23}$$

This expression approaches two simple limiting values

$$R_i = \begin{cases} (\alpha_1^2 \frac{1}{2} c_f)^{-1} (\frac{3}{2})^2, & \text{for } U_g >> U_a \\ (\alpha_1^2 \frac{1}{2} c_f)^{-1} (\frac{U_g}{U_a})^2, & \text{for } U_g << U_a \end{cases} \tag{2.24}$$

The cloud height variation may then be approximated from Eguation (2.16) as

$$\frac{dh}{dt} \simeq \frac{dh_d}{dt} \propto \begin{cases} \alpha_1^2 \alpha_4 (\frac{1}{2} c_f)^{3/2} U_g, & \text{for } U_g >> U_a \\ \alpha_6 (\frac{1}{2} c_f)^{1/2} U_a, & \text{for } U_g << U_a \end{cases} \tag{2.25}$$

In the limit as $t >> t_I$, U_g will aproach zero so that the lower of these limits is almost always the most realistic. Integration gives

$$h(t) \simeq \alpha_6 (\frac{1}{2} c_f)^{\frac{1}{2}} U_a (t-t_o) \tag{2.26}$$

$$\simeq \alpha_6 w_m (t-t_o)$$

The prediction inaccuracy for vertical diffusion of passive scalar clouds is,as summarized by Hanna et al. (26),large. The simple law above is, therefore, judged to be accurate enough as an asympthotic limit for heavy gas dispersion.

Equation (2.26), combined with Equation (2.6) for r(t), results in a limiting concentration decrease:

$$c \propto \begin{cases} t^{-2} & \text{, for instantaneous source} \\ x^{-3/2} & \text{, for continuous source} \end{cases} \qquad (2.27)$$

2.4 Thermodynamics

It is expected (6) that the most important heat transfer takes place in the initial stages of the cloud development. Our model for this stage is incomplete, so that a complicated description of the thermodynamics is not consistent. Although the gas mixture is in motion and may be far from beeing in thermodynamic equilibrium, the static pressure, p, is assumed to be constant and the ideal gas law assumed to be valid

$$\rho = \frac{P}{RT} \qquad (2.27)$$

When the universal gas constant is R, the "gas constant" for a gas with molecular weight m_i is $R_i = R/m_i$. The specific heat at constant pressure is roughly estimated as $c_{pi} \simeq 7/2 \cdot R_i$. For a mixture of two ideal gasses:

$$R(t) = \frac{M_g R_g + M_a(t) R_a}{M_a + M_a(t)} \qquad (2.28)$$

$$c_p(t) = \frac{M_g\, c_{pg} + M_a\, c_{pa}}{M_g + M_a(t)} \qquad (2.29)$$

For the continuous source case, the corresponding equations are obtained by replacing the M_i's by dM_i/dt.

2.4.1 Enthalpy equation

The fraction of the liquid mass thrown into the air-gas mixture as droplets during the release, δ, is evaporated there. Depending upon the type of gas and release, this fraction may vary from almost zero to close to one (7). The temperature of the cloud will not rise much until enough warm air has been entrained to evaporate the droplets. The necessary amount of entrained air M_{ad}, is

$$M_{ad}\left[c_{pa}(T_a-T_g) + L_w\,\chi_w\right] \simeq \delta \cdot M_g \cdot L_g \qquad (2.30)$$

Here χ_w is the mass mixing ratio of water vapour, L_w the latent heat of evaporation or sublimation of water, and L_g the latent heat of the gas. When the droplets are evaporated, the temperature of the cold cloud rises. As there is disagreements on the enthalphy equation to be used (4,6,7), we will present arguments for our (simple) choice (6). We assume that the entrained air mass ΔM_a, over the time interval Δt, is mixed instantaneously into the homogeneous gas cloud. The enthalpy ,H, before and after the mixing is then

$$H(t) = M(t)c_p(t)T(t) + c_{pa}\,T_a\,\Delta M_a \qquad (2.31)$$

$$\begin{aligned} H(t+\Delta t) &= M(t+\Delta t)c_p(t+\Delta t)T(t+\Delta t) \\ &= M(t)c_p(t) + c_{pa}\,\Delta M_a\,T(t+\Delta t) \\ &= M(t)c_p(t)T(t+\Delta t) + c_{pa}T(t)\,\Delta M_a \end{aligned} \qquad (2.32)$$

The enthalpy increase is equal to the heat transfer

$$\frac{H(t+\Delta t) - H(t)}{\Delta t} = \pi r^2\,\frac{\Delta q}{\Delta t} \qquad (2.33)$$

Substitution from Equations (2.31) and (2.32) into (2.33) gives, in the limit as $\Delta t \to 0$:

$$M(t)c_p(t)\frac{dt}{dt} + c_{pa}(T-T_a)\frac{dM_a}{dt} = r\frac{dq}{dt} \qquad (2.34)$$

Use of the Equations (2.1a) and (2.12a) gives

$$h\frac{dT}{dt} = \frac{1}{\rho c_p}\frac{dq}{dt} + (T_a-T)\frac{\rho_a c_{pa}}{\rho c_p}\left(\frac{dh}{dt}\right)_* \qquad (2.35)$$

The heat transfer is in the form of sensible heat from the warm underlying surface, and as latent heat from the condensed water vapour. Since there is an imposed gravity flow field, U_g, we assume that the sensible heat transfer from the surface may be approximated by forced convection heat transfer, as described by for instance Welty et al. (27). The heat transfer per unit area is proportional to the difference between the surface temperature $T_a(0)$, and the gas temperature, T:

$$\left(\frac{dq}{dt}\right)_s \simeq St\cdot\rho\cdot c_p\, U(T_a(0)-T) \qquad (2.36)$$

It is assumed that the conductivity of the surface is sufficiently high to keep $T_a(0)$ approximately constant. The Reynolds analogy, stating that the coefficients of heat and momentum transfer are approximately equal, is used to approximate the Stanton number, St.

$$St \simeq \tfrac{1}{2} c_f \qquad (2.37)$$

The heat transfer from the surface must be equal to the turbulent enthalpy flux near the surface so that

$$(\overline{\theta w})_0 = \tfrac{1}{2} c_f\, U(T_a(0) - T) \qquad (2.38)$$

The latent heat transfer is

$$\left(\frac{dq}{dt}\right)_L = L_w \chi_w \rho_a \left(\frac{dh}{dt}\right)_* H(T_{da}-T) \tag{2.39}$$

Here $H(T_{da}-T)$ is the Heavyside generalized unit function, and T_{da} is the dew point temperature. The mixing ratio of water vapour is obtained from the Clausius-Clapeyron equation

$$\chi_w \simeq 3.7 \cdot 10^{-3} \exp \frac{L_w}{R_w} \left(\frac{1}{273} - \frac{1}{T_{da}}\right) \tag{2.40}$$

Although χ_w is normally very small, the moisture term cannot generally be neglected in Equation (2.35). The enthalphy equation may then be written as:

$$\frac{dT}{dt} = \frac{1}{h} \left[(\overline{\theta w})_o - (\overline{\theta w})_h \right] \tag{2.41}$$

with

$$(\overline{\theta w})_h = \left[(T_a - T) + \frac{L_w}{c_{pa}} \chi_w H(T_{da}-T) \right] \frac{\rho_a c_{pa}}{\rho c_p} \left(\frac{dh}{dt}\right)_* \tag{2.42}$$

If the air necessary to evaporate the droplets, M_{ad}, is not entrained during the release process, the enthalphy equation (2.41) is modified by a Heavyside weight function

$$\frac{dT}{dt} \simeq \frac{1}{h} \left[(\overline{\theta w})_o - (\overline{\theta w})_h \right] H(M_a(t) - M_{ad}) \tag{2.43}$$

Lacking a realistic release model, it is assumed here that the amount of air necessary to evaporate the droplets is available, $M_a(0) = M_{ad}$. The set of equations to describe the heavy gas flow is now closed. The equations are ordinary, nonlinear differential equations expected to be integrable as long as $\rho(t) > \rho_a$. We have not been able to find analytical solutions and have used the Runge-Kutta-Mersion method for integration (Skjeldestad (27)). The following variables are kept constant: $g = 10\ ms^{-2}$; $m_a = 29$ g/mol; $R_* = 8.3$ J/mol·deg; $L_w = 2.5 \cdot 10^6$ J/kg; $\rho_a = 1.3$ kg m^{-3}; $T_a = 283$, $T_a - T_{da} = 5$.

2.5 Sensitivity analysis

It is essential that model predictions do not vary too much when the coefficients are varied over their normal range of uncertainty. As we have seen, the coefficient variations may be contained in α_1, α_2, α_4, α_5, and α_6. As both α_1 and α_6 affect the cloud development in a simple way, the most interesting variability may be discussed in terms of the three coefficients $\alpha_2 \varepsilon (0.2, 1.0)$, $\alpha_4 \varepsilon (0.2, 5.0)$ and $\alpha_5 \varepsilon (0.1)$.

Figure 2.1 illustrates a representative variation of cloud state for two different values of the initial entrainment coefficient, α_5. It is indicated that the entrainment equation (2.15) affects the dispersion significantly only in the initial stages. The prediction of the cloud state at the end of the slumping stage is not critically dependent on the entrainment coefficient α_5.

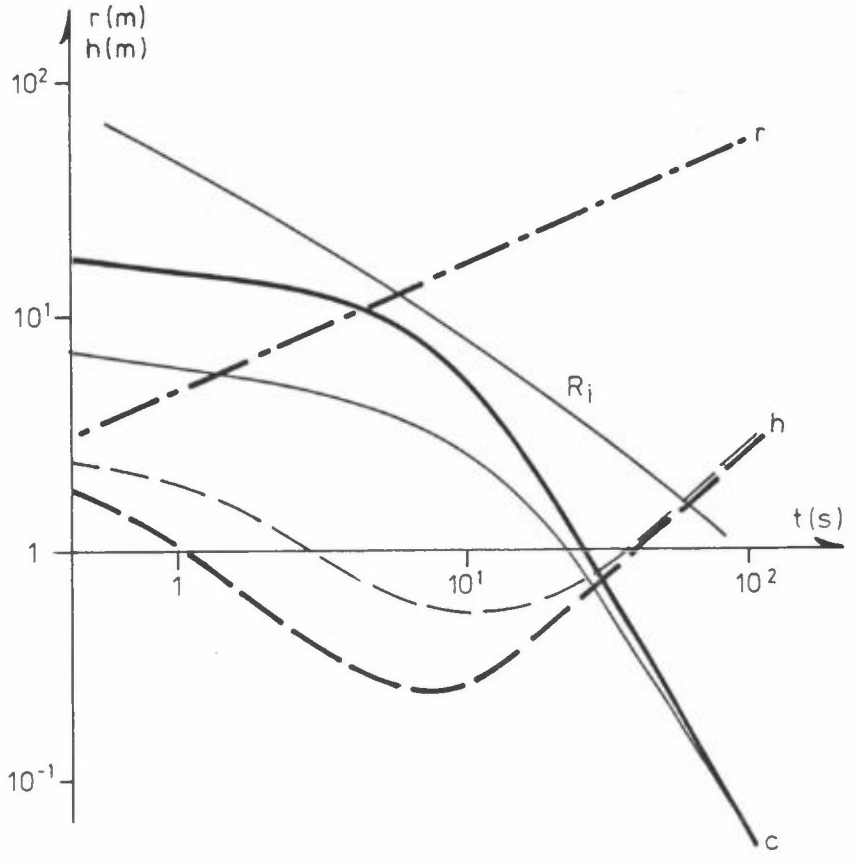

Figure 2.1: Variation of initial entrainment. Heavy curves: $\alpha_5 = 0.5$. Thin curves: $\alpha_5 = 1.0$ Release of $V(o) = 49\ m^3$ freon-air mixture $\rho(o)/\rho_a = 2$, $h(o)/r(o) = 1.84$, $T_o = T_a$, $U_o = 2\ ms^{-1}$ $c_f = 1.4 \cdot 10^{-3}$, $\alpha_1 = 1.4$, $\alpha_2 = 0.7$, $\alpha_3 = 1.3$, $\alpha_4 = 2.5$, $\alpha_6 = 0.3$.

Figure 2.2 illustrates a representative variation of cloud state for two different values of the entrainment coefficient, α_4. It is indicated that the entrainment equation (2.16) affects the dispersion significantly only after the initial stages. The predicted state of the cloud is not critically dependent on the coefficient α_4.

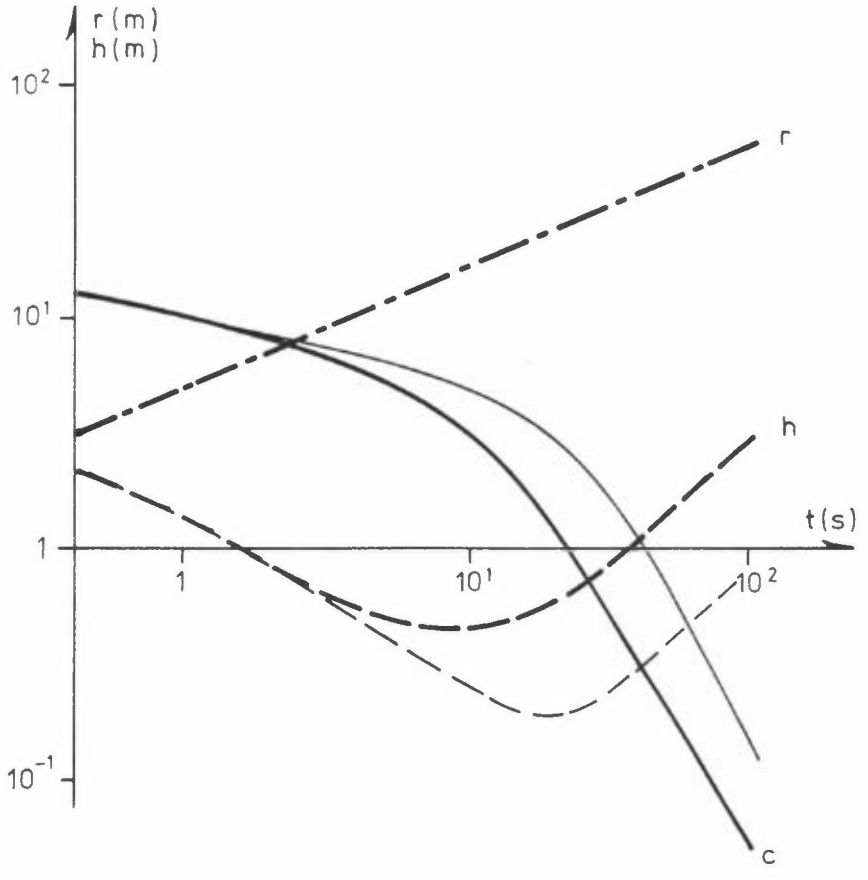

Figure 2.2: Variation of eventual entrainment.
Heavy curves: $\alpha_4 = 5.0$. Thin curves: $\alpha_4 = 0.2$.
Release of $V(o) = 40\ m^3$ freon-air mixture. $\rho(o)\rho_a = 2$, $h(o)/r(o) = 1.84$, $T_G = T_a$; $U_a = 2\ ms^{-1}$, $c_f = 1.4 \cdot 10^{-2}$, $\alpha_1 = 1.4$, $\alpha_2 = 0.7$, $\alpha_3 = 1.3$, $\alpha_5 = 0.8$, $\alpha_6 = 0.3$.

Figure 2.3 illustrates the variation of cloud state for two different values of the coefficient α_2 to characterize the importance of the convective turbulence in relation to mechanical turbulence. The gas chosen is methane to maximize the effect of heat transfer. The predicted state of the cloud is dependent, but not critically dependent on α_2.

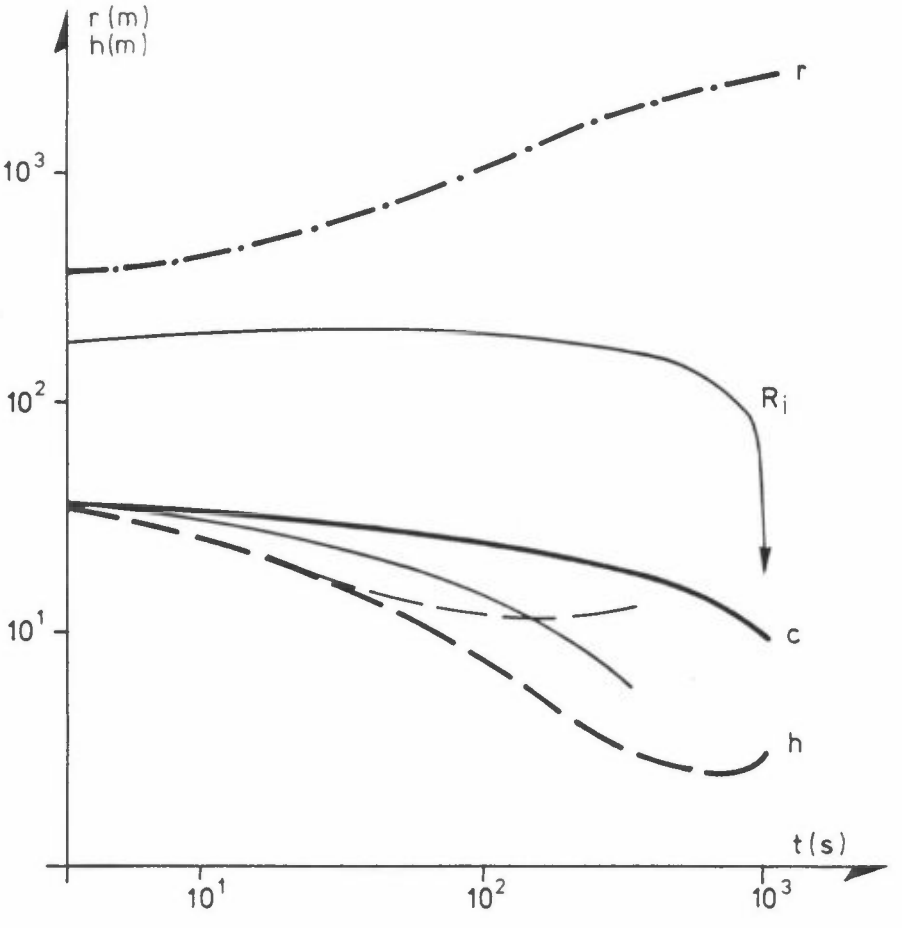

Figure 2.3: Variation of convective entrainment.
Heavy curves: $\alpha_2 = 0.5$. Thin curves: $\alpha_2 = 1.5$.
Release of 10^7 kg methane at boiling temperature.
$\delta = 0.5$, $h(o)/r(o) = 0.25$. $U_a = 0.5\ ms^{-1}$, $c_f = 2 \cdot 10^{-3}$,
$T-T_a = 5$, $\alpha_1 = 1.3$, $\alpha_3 = 1.3$, $\alpha_4 = 3.5$, $\alpha_5 = 0.5$,
$\alpha_5 = 0.3$.

It is therefore concluded that if reasonably chosen coefficient enable the model to explain interesting aspects of experimental data on heavy gas dispersion, there is reason to believe that the model is physically realistic. The traditionally accepted coefficients are: $\alpha_1 = 1.3$, $\alpha_2 = 0.7$, $\alpha_3 = 1.3$, $\alpha_4 = 3.5$, and $\alpha_6 = 0.3$. The ad hoc coefficient $\alpha_5 = 0.5$ is chosen so as not to give too large initial entrainment.

3 DATA COMPARISON

The Porton experiments (11) contain the bulk of the quantitative experimental data on the spreading of heavy gases in the atmosphere. The field experiments were carried out with an instantaneous source of 40 m^3 volume of gas mixture, which had densities in the range of 1.03 to 4.2 relative to air. The gas temperature was equal to the atmospheric temperature. Orange smoke was used to make the cloud visible. The cloud dispersion was monitored by side-view and plan-view photographs, by gas dosage measurements and by continuous measurements of gas concentration.

We use the data from the flat sites only. Using the friction velocity and mean wind speed for each experiment, the estimated friction coefficient at the different flat sites are as follows: $z_o = 2$ mm $\rightarrow c_f \simeq 7 \cdot 10^{-3}$; ($z_o = 10$ mm, $z_o = 20$ mm) $\rightarrow c_f \simeq 1.4 \cdot 10^{-2}$ and $z_o = 150$ mm $\rightarrow c_f = 5 \cdot 10^{-2}$. These groups contain 10, 18 and 3 experiments respectively. Neither Picknet (11) nor we have discovered, from the data, any significant dependence between dispersion variables and surface roughness. In the following, we will therefore only use $c_f = 1.4 \cdot 10^{-2}$ for model predictions.

The variables used to characterize the cloud were its height, downwind and crosswind cloud dimensions, and the average volume concentration (11). The difference between the downwind and crosswind cloud dimensions, caused by the combined effect of turbulence and mean wind shear, is not too large and cannot be discribed by our model. The observed crosswind cloud size is

associated with the predicted 2r. As most of the gas mass may be contained in a intense vortex ring (11) it must be difficult to estimate a representative cloud height. The observed height h_*,could be more representative for the ring than for the whole cloud. Redistribution of the mass from the circumferential ring of radius ($h_*/2$) evenly over the cylindrical cloud of radius r gives a cloud height of ($2\pi/4 \cdot h_*^2/r$). In the neighbourhood of its minimum, h_* is observed to be of the order 1/10 r, so that a representative height could sometimes have been overestimated by a factor of 10. This difference is illustrated in Figure 3.1. The ambiguity will affect the concentration curves linearly so that a representative concentration may sometimes have been underestimated by a factor of about 10.

The predicted cloud development resembles very much the observed one, are illustrated in Figures 2.1, 2.2 and 3.1. The largest discrepancy is apparently between the observed and predicted cloud height, illustrated in Figure 3.1. This apparent discrepancy could easily been made much smaller, without large increase of other types of errors, by using a larger initial entrainment

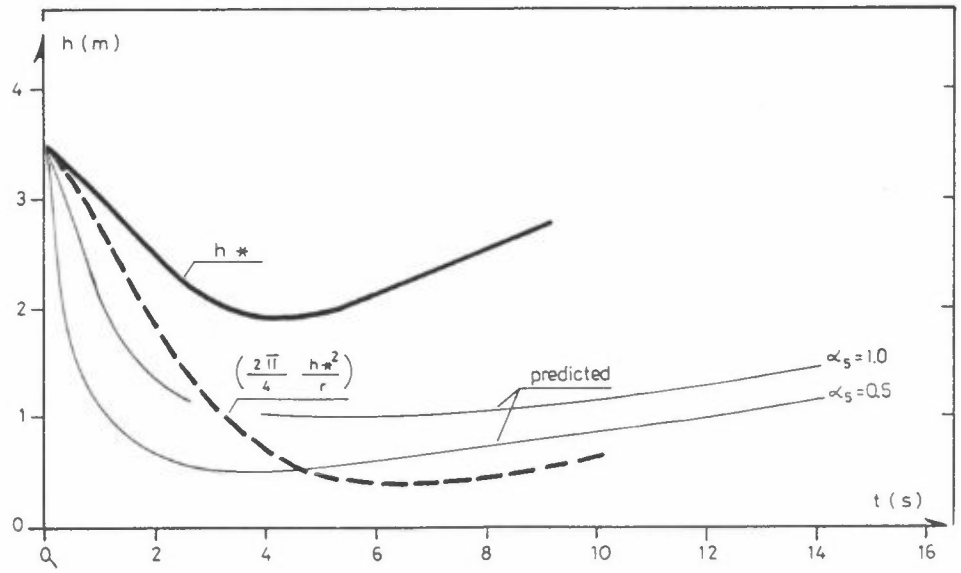

Figure 3.1: Mean observed and "corrected" height variation for the Porton experiments no: (13,20,28,37), and predicted variation for α_s = 0.5 and α_s = 1.0. $\rho(o)/\rho_a$ = 2.15, U_a = 5.4 ms^{-1}, c_f = $1.4 \cdot 10^{-2}$.

coefficient, α_5. However, because the discrepancy may not be real, or also because the initial entrainment in the Porton experiments could be nonrepresentative due to the particular gas release mechanism α_5 is not chosen to minimize this (apparent?)error.

With a general agreement between the actual and predicted cloud development, the data may be represented in terms of a few variables instead of functions. We choose: time to minimum cloud height $t(h_{min})$, transverse cloud dimension, $2r(t=10$ sec), and volume concentration $c(t=10$ sec).

Most of the Porton experiments were associated with reasonably high winds. As illustrated in Figure 2.1, the spreading will then occur at reasonably small Richardson numbers, and therefore approach passive scalar dispersion when $t > 0$ (10 sec). The most dominant variations of the three dispersion variables are shown in the Figures 3.2, 3.3 and 3.4. Predicted isolines are also shown. Considering the simplicity of the model, the complexity of the heavy gas process, the uncertainty of the coefficients and the randomness and possible bias associated with the data, the similarity between the predicted and actual values is judged to be remarkable.

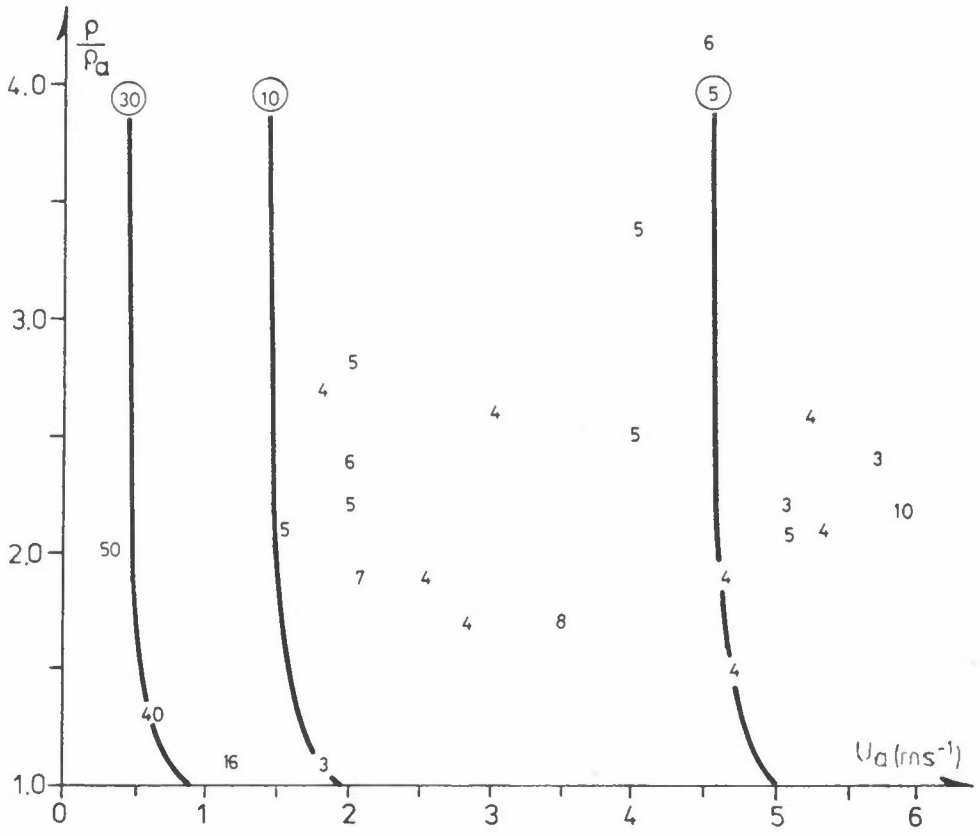

Figure 3.2: Portion data for time in seconds to minimum cloud height. Isocurves for predicted values $c_f = 1.4 \cdot 10^{-2}$, $\alpha_1 = 1.3$, $\alpha_2 = 0.7$, $\alpha_3 = 1.3$, $\alpha_4 = 3.5$, $\alpha_5 = 0.5$, $\alpha_6 = 0.3$.

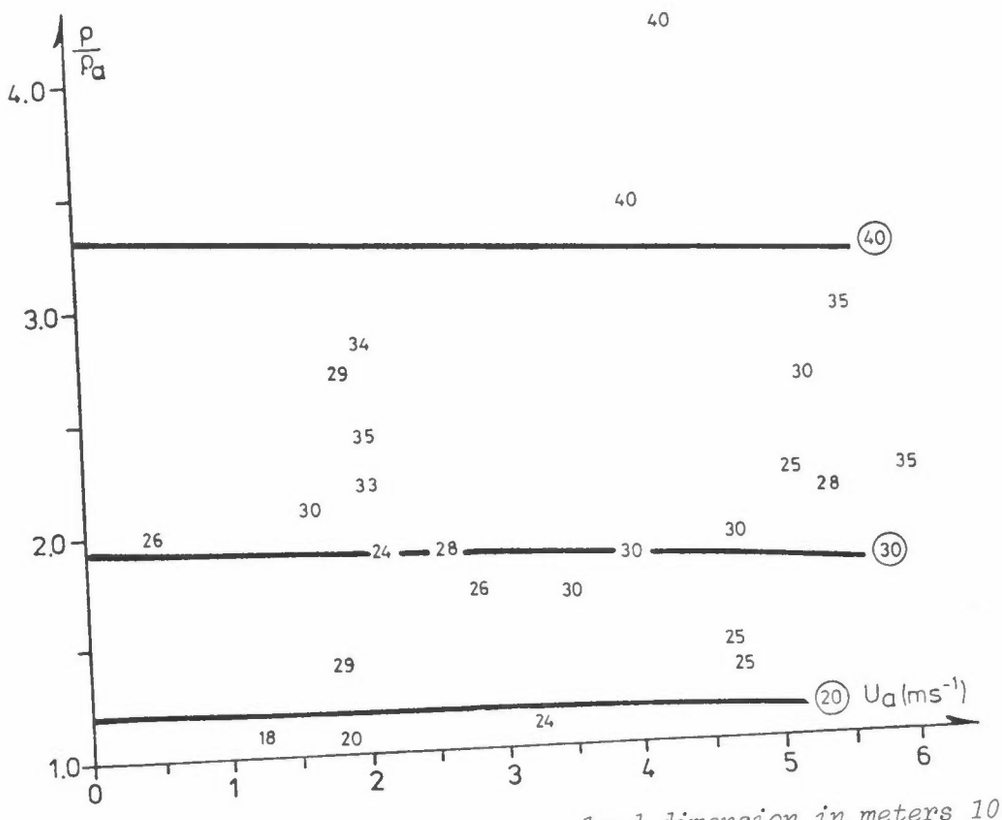

Figure 3.3: Porton data for transverse cloud dimension in meters 10 sec from release. Isocurves for predicted values. $c_f = 1.4 \cdot 10^{-2}$, $\alpha_1 = 1.3$, $\alpha_2 = 0.7$, $\alpha_3 = 1.3$, $\alpha_4 = 3.5$, $\alpha_5 = 0.5$, $\alpha_6 = 0.3$.

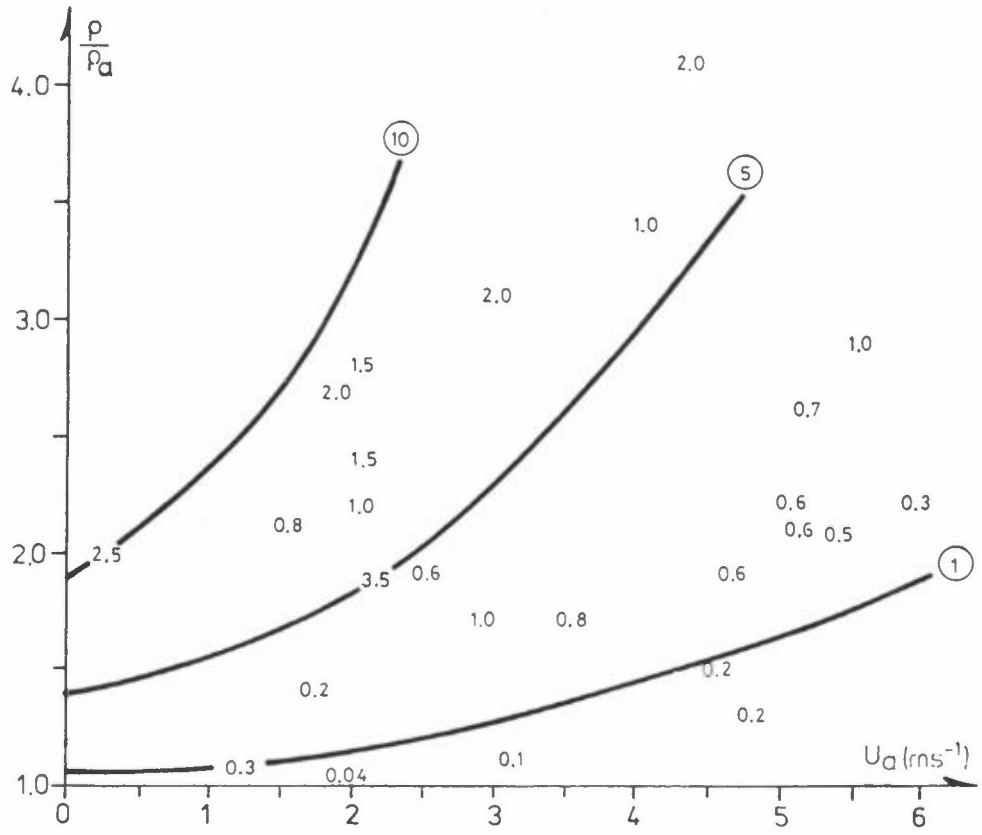

Figure 3.4: Porton data for volume concentration in percent 10 sec from release. Isocurves for predicted values $c_f = 1.4 \cdot 10^{-2}$, $\alpha_1 = 1.3$, $\alpha_2 = 0.7$, $\alpha_3 = 1.3$, $\alpha_4 = 3.5$, $\alpha_5 = 0.5$, $\alpha_6 = 0.3$.

4 PREDICTED SPREAD

The simple model has been found to be well conditioned and to explain important aspects of the very sparce experimental data on heavy gas dispersion. The experimental data cover only "points" in the phase space spanned by probable release and environmental conditions. It is of interest to discuss the model prediction over a portion of this space of more relevance to hazard.

Figure 4.1 illustrates the variation of the "hazard" variables, t(c=1%) and r(c=1%) with released mass of propane. The approximate relations, obtained from Figure 4.1, show that the variations with the released mass are slow.

$$t(c=1\%) \propto M_g^{1/3} \qquad (4.1)$$

$$r(c=1\%) \propto M_g^{2/5+} \qquad (4.2)$$

Figure 4.2 illustrates the variation of the variables t(c=1%) and r(c=1%) with the ammount of liquid evaporated initially in the air-propane mixture. There is practically no dependence. The variation with initial cloud shape, h(o)/r(o), was also found to be small. As illustrated in Figure 4.2, the spread of a methane cloud is somewhat more dependent upon the ammount of liquid evaporated in the air. However, for the small, most realistic values of δ, the dependence is not decisive.

Environmental variations are illustrated in Figure 4.3. There is a large variation of the variables t(c=1%) and r(c=1%) with both wind speed and the roughness of the underlying surface. The maximum "hazard" distance, x(c=1%), of the order

$$x(c=1\%) \simeq U_a \; t(c=1\%) + r(c=1\%) \qquad (4.3)$$

shows a remarkably small variation with the wind speed. With other conditions kept constant, the hazard from a heavy gas release is more serious in calm wind conditions, mainly because t(c=1%) is high.

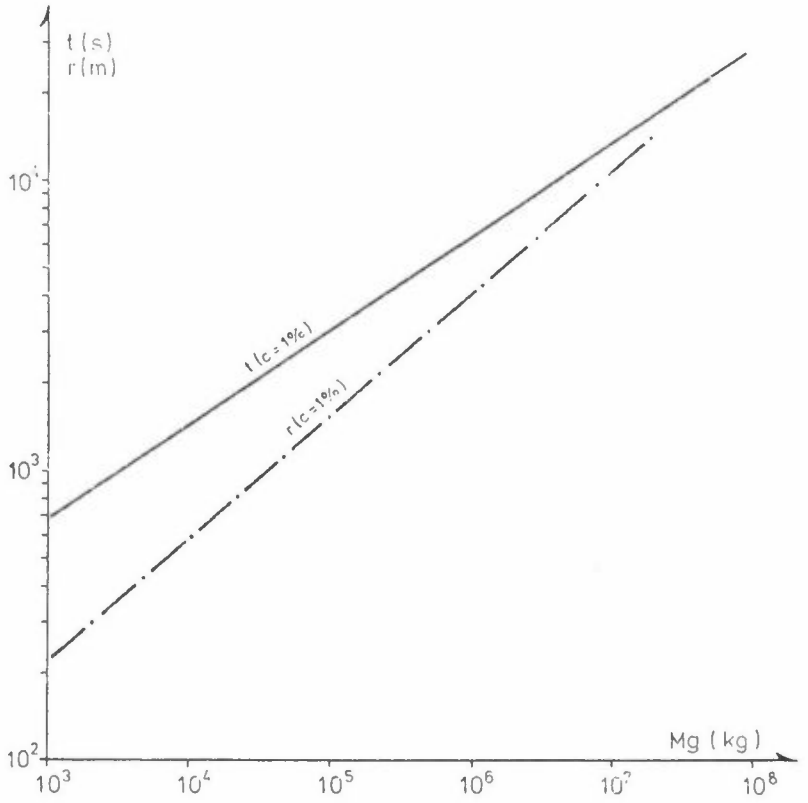

Figure 4.1: Propane mass variation. Time to and radius at 1% mass concentration as functions of released mass. $\delta = 0.1$, $h(o)/r(o) = 0.25$, $c_f = 2 \cdot 10^{-3}$, $U_a = 0.5\ ms^{-1}$, $T-T_d = 5$, $\alpha_1 = 1.3$, $\alpha_2 = 0.7$, $\alpha_3 = 1.3$, $\alpha_4 = 3.5$, $\alpha_5 = 0.5$, $\alpha_6 = 0.3$.

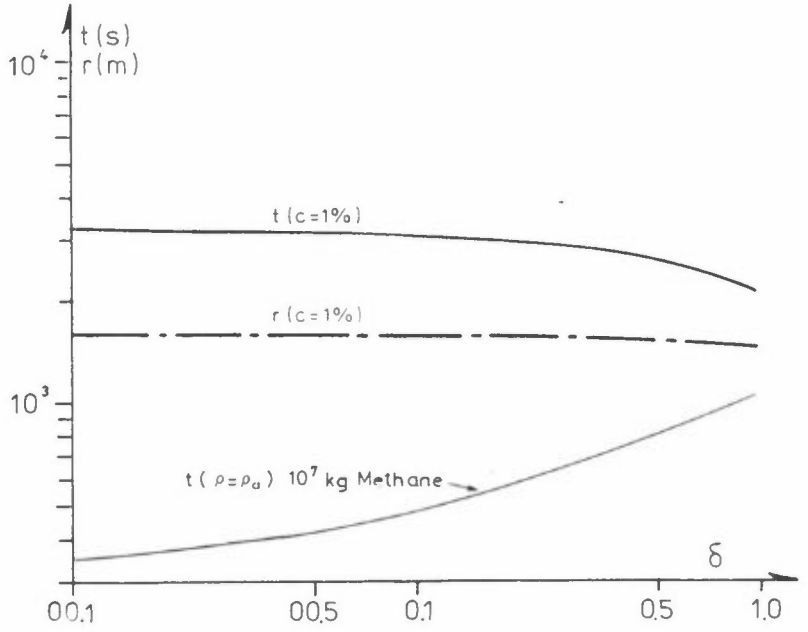

Figure 4.2: Evaporation of aerosol. Time to and radius at 1% mass concentration as function of the mass ratio evaporated in the air-propane cloud. $M_g = 10^5$ kg, $h(o)/r(o) = 0.25$, $c_f = 2 \cdot 10^{-3}$, $U_a = 0.5\ ms^{-1}$, $T-T_d = 5$, $\alpha_1 = 1.3$, $\alpha_2 = 0.7$, $\alpha_3 = 1.3$, $\alpha_4 = 3.5$, $\alpha_5 = 0.5$, $\alpha_6 = 0.3$.

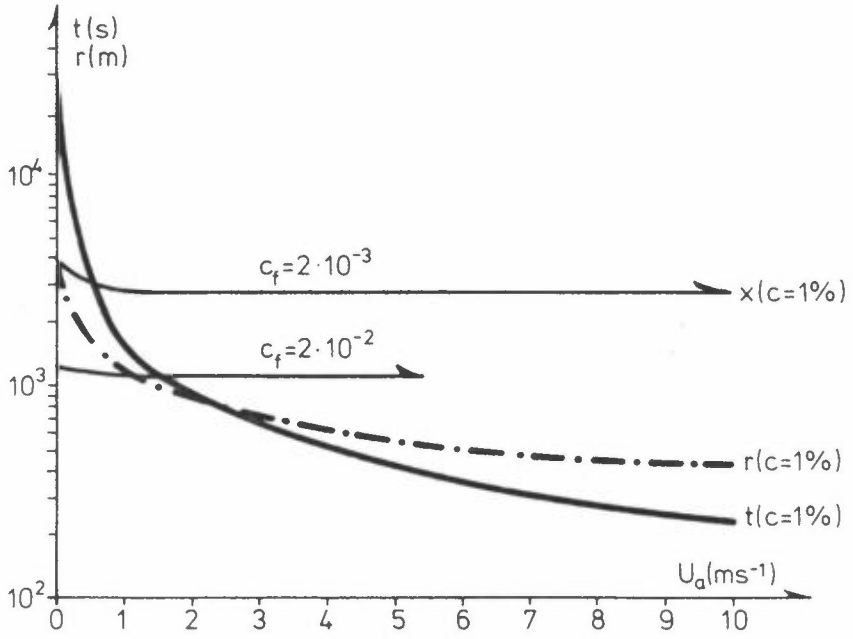

Figure 4.3: Environmental variations. "Hazard" variables as function of wind speed and surface roughness. Propane, $M_g = 10^5 kg$, $\delta = 0.1$, $h(o)/r(o) = 0.25$, $\alpha_1 = 1.3$, $\alpha_2 = 0.7$, $\alpha_3 = 1.3$, $\alpha_4 = 3.5$, $\alpha_5 = 0.5$, $\alpha_6 = 0.3$.

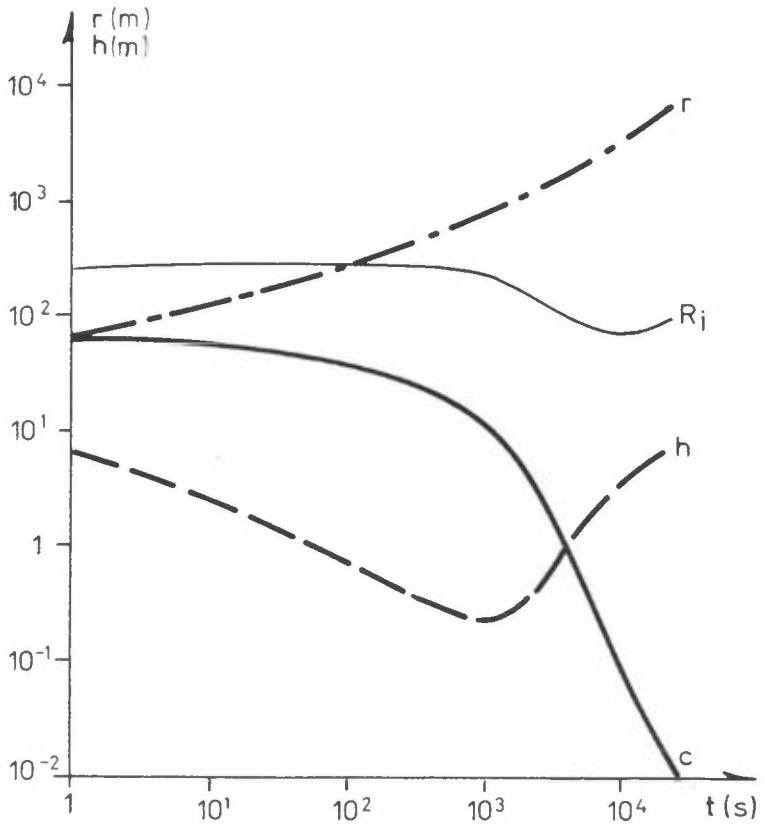

Figure 4.4: Spread of chlorine to small concentrations. No predicted significant variations with atmospheric stratification, $M_g = 10^5 kg$, $\delta = 0.1$, $h(o)/r(o) = 0.25$. $U_a = 0.5\ ms^{-1}$, $c_f = 2\cdot10^{-3}$. $\alpha_1 = 1.3$, $\alpha_2 = 0.7$, $\alpha_3 = 1.3$, $\alpha_4 = 3.5$, $\alpha_5 = 0.5$, $\alpha_6 = 0.3$.

For temperatures in the neighbourhood of $10^{o}C$, there are only small predicted variations of the dispersion with the water vapour content. Even for the spreading and dilution of clorine to small concentrations, as shown in Figure 4.3, the predicted variations with the stratification of the atmosphere, $\partial T_a/\partial z$ are negligible. However, it should be noted that the variation of atmospheric stratification has only been included in the $\Delta\rho$ and $(T-T_a)$ terms. The associated change of atmospheric turbulence has not been taken into account.

5 CONCLUDING REMARKS

We have tried to describe the dynamics of the most essential state variables of a heavy gas cloud as simply as possible. Possible refinements of some approximations are obvious, but the design of a consistent and significantly more realistic model seem to introduce complications. The complications are accociated with for instance: The coupling between the release and entrainment processes, the coupling between the atmospheric flow and the gravity indused flow, and the spatial variations of the gas cloud characteristica.

The present model is attractive in that the results do not depend critically upon uncertainties about numerical coefficients. With an ad hoc initial entrainment equation, the model gives a remarkably accurate prediction of the Porton experimental data, which constitute the bulk of the existing data on heavy gas dispersion.

The potential hazard of a large (accidental) gas release is predicted to vary significantly with the state of the underlying surface and atmosphere, especially so in the neighbourhood of the potentially most hazardous conditions; small wind speed. The statistics of hazard is therefore closely related to the statistics of environmental states.

ACKNOWLEDGEMENT

The constructive critism received from Dr. H. Tennekes on an early version of this manuscript, is appreciated.

5 REFERENCES

(1) Fay, V.A. — Unusual fire hazard of LNG tanker spills. *Combust. Sci. Technol.*, 7, 47-49 (1973).

(2) van Ulden, A.P. — On the spreding of a heavy gas released near the ground. *I: 1st international loss prevention symposium*. The Hague/Delft, Netherlands 28-30 May 1974. Amsterdam, Elsevier, 1974, pp. 221-226, 431-439.

(3) te Riele, P.H.M. — Atmospheric dispersion of heavy gases emitted at or near ground level. *I: 2nd international loss prevention symposium*. Heidelberg 6-9 Sept. 1977, pp 347-357.

(4) Germeles, A.E. Drake, E.M. — Gravity spreading and atmospheric dispersion of LNG vapour clouds. *I: The 4th int. symposium on transport of hazardous cargoes by sea and inland waterways*. Jacksonville, Florida, 1975, pp. 519-539.

(5) — LNG terminal risk assessment study for point conception, California. La Jolla, Calif., Science Application, 1976.

(6) Eidsvik, K.J. — Dispersion of heavy gas clouds in the atmosphere. Lillestrøm 1978. (NILU OR 32/78.)

(7) Kaiser, G.D. Walker, B.C. — Releases of anhydrous ammonia from pressurized containers. *Atmos. Environ.* 12, 2289-2300 (1978).

(8) Burges, D. Biordi, J. Murphy, J. — Hazards of spillage of LNG into water. Pittsburg, Pa, Bureau of Mines, 1972. (PMSRC Rep.no 4177.)

(9) Feldbauer, G.F.
Heigl, J.J.
Mc Queen, W.
Mag, W.G.
Spills of LNG on water - "Vaporization & downwind drift of combustible mixtures". Florham Park, Esso Research & Engineering Company, 1972. (Report no EEGIE-72.)

(10)
LNG safety program interim report on phase II work. Columbus, Ohio, Battelle, 1974. (American Gas Association Project IS-3-1.)

(11) Picknett, R.G.
Field experiments on the behaviour of dense clouds. Salisbury, Wilts., England, Chemical Defence Establishment Porton Down 1978. (Report Ptn. IL 1154/78/1.)

(12) Donaldson C.
Bilanin, A.J.
Vortex wakes of conventional aircraft. Neuilly Sur Seine 1975 (AGARD-AG-204).

(13) Deardorff, U.W.
Three-dimensional numerical study of the height and mean structure of a heated planetary boundary layer. *Boundary-Layer Meteorol.* 7 , 81-106 (1974).

(14) Monin, A.S.
Yaglom, A.M.
Statistical fluid mechanics; mechanics of turbulence. Vol. 1. Cambridge, Mass., The MIT Press, 1971.

(15) Kato, H.
Phillips, O.M.
On the penetration of a turbulent layer into a stratifield fluid. *J.Fluid Mech.* 37, 643-655 (1969).

(16) Crapper, P.E.
Linden, P.F.
The structure of density interfaces. *J.Fluid Mech.* 65, 45-63 (1973).

(17) Wu, J.
Wind - indused turbulent entertainment across a stable density interface. *J. Fluid Mech.* 61, 257-287 (1973).

(18) Tennekes, H.
A model for the dynamic of the inversion above a convective boundary layer.
J.Atmos.Sci. 30, 558-567 (1973).

(19) Heidt, F.D.
The growth of the mixed layer in a stratified fluid due to penetrative convection.
Boundary Layer Meteorol. 12, 439-461 (1977).

(20) Zeman, O.
Tennekes, H.
Parameterization of the turbulent energy budget at the top of the daytime. Atmospheric boundary layer.
*J.Atmos. Sci.*34, 111-123 (1977).

(21) Long, R.K.
Some aspects of turbulence in geophysical systems.
Adv.in appl. mech. 17, 1-90 (1977).

(22) Long, R.K.
A theory of mixing in a stably stratified fluid.
J.Fluid Mech. 84, 113-124 (1978).

(23) Tennekes, H.
Lumley, J.L.
A first course in turbulence.
Cambridge, The MIT - Press, 1972.

(24) Kitaigorodskii, S.A.
The analysis of air-sea interaction.
Jerusalem, Israel program for scientific translations, 1973.

(25) Hanna, S.R.
Briggs, G.A.
Deardorff, B.A.
Egan, B.A.
Gifford, F.A.
Pasquill, F.
AMS workshop on stability classification schemes and sigma curves - summary of recommendations.
Bull.Am.Meteorol.Soc. 58, 1305-1309 (1977).

(26) Welty, J.R.
Wilks, C.E.
Wilson, R.E.
Fundamentals of momentum, heat and mass transfer.
New York, Wiley, 1969.

(27) Skjeldestad, K.
DAREP - Users manual. Kjeller 1977. (Norwegian Defence Research Establishment. Teknisk notat S-465.) (In Norwegian).

NORSK INSTITUTT FOR LUFTFORSKNING
(NORGES TEKNISK-NATURVITENSKAPELIGE FORSKNINGSRÅD)
POSTBOKS 130, 2001 LILLESTRØM
ELVEGT. 52.
TLF. (02) 71 41 70

RAPPORTTYPE Oppdragsrapport	RAPPORTNR. 18/79	ISBN--82-7247-113-2
DATO Juni 1979	ANSV.SIGN. O.Fd.	ANT.SIDER OG BILAG 39
TITTEL A model for heavy gas dispersion in the atmosphere		PROSJEKTLEDER K.J. Eidsvik NILU PROSJEKT NR 25077
FORFATTER(E) K.J. Eidsvik		TILGJENGELIGHET ** A OPPDRAGSGIVERS REF.
OPPDRAGSGIVER NTNF		
3 STIKKORD (á maks.20 anslag) Tunge gasser | Spredning i luft		Eksplosive gasser

REFERAT (maks. 300 anslag, 5-10 linjer)

Rapporten beskriver en enkel modell for spredningen av en tung og kald gass-sky i atmosfæren. Resultatet er ikke kritisk avhengig av koeffesientvariasjoner. Beregnet spredning passer godt med spredningsdata fra Porton.

TITTEL A model for heavy gas dispersion in the atmosphere

ABSTRACT (max. 300 characters, 5-10 lines)

A simple model for the sispersion of heavy and cold gas cloud is developed. The results are not critically dependent upon coefficient variations. The predicted spread show good correspondence with data from Porton.

**Kategorier: Åpen - kan bestilles fra NILU A
Må bestilles gjennom oppdragsgiver B
Kan ikke utleveres C